ECCOMAS Congress 2016
VII European Congress on Computational Methods in Applied Sciences and Engineering
M. Papadrakakis, V. Papadopoulos, G. Stefanou, V. Plevris (eds.)
Crete Island, Greece, 5–10 June 2016

STATISTICAL AND GEOMETRICAL CHARACTERISTICS OF RANDOMLY ROUGH SURFACES USED FOR CONTACT SIMULATIONS.

Rafael Schouwenaars[1], Carlos G. Figueroa[1], Víctor H. Jacobo[1] and Armando Ortiz[1]

[1] Departamento de Materiales y Manufactura
Facultad de Ingeniería Edif. O
Universidad Nacional Autónoma de México
Avenida Universidad 3000, CDMX
e-mail: raf_schouwenaars@yahoo.com, vicjacobo@yahoo.com.mx, armandoo@unam.mx

Keywords: Contact mechanics, Fractal surface, Finite elements, Midpoint algorithm, Spectral method.

Abstract. *Over the last decades, it has been established that rough surfaces of technological materials can be described by means of random processes with fractal character. This means that the numerical simulation of contact mechanics will depend on the size of the simulated surface or the lower cut-of distance (i.e. mesh size) of the simulation; moreover, each simulation only presents a single case out of an infinite spectrum of possible results. This work explores the problem of statistical convergence by focusing on the surface characteristics which are relevant for contact mechanics applications, i.e. the amount of simulations required to obtain a reasonable estimate of the surface characteristics as a function of the size of the simulated surface. This analysis is applied to three classical methods for the generation of fractal surfaces, i.e. the Midpoint Displacement algorithm, the generalised Weierstrass-Mandelbrot function and a Random Spectral method. Apart from geometrical characteristics, the simulated surfaces will be evaluated by means of a numerical modification of the Greenwood-Williamson model. It will be seen that the Weierstrass-Mandelbrot function has several shortcomings which may affect advanced contact simulations. More generally, the statistical variation between individual surface simulations introduces a considerable spread on the results, as seen in the distribution of calculated fractal dimensions or load-contact area curves.*

1 INTRODUCTION

The random nature of the roughness of engineering surfaces and its role in the determination of contact problems has been recognised since the middle of the 20th century. Archard [1] postulated a model consisting of superimposed elastic spheres of decreasing size to approximate a rough elastic surface. Greenwood and Williamson (GW) [2] in 1966 formulated their contact model in which randomly distributed asperities were modelled as spherical caps. Their model was random but not fractal. Likewise, in 1969, Whitehouse and Archard [3] provided an advanced statistical analysis of the asperity distribution for a randomly rough surface modelled as white noise.

Independently, Longuet-Higgins [4] in 1957 analysed the random superposition of waves of different frequencies as a model for the sea surface and provided an analysis of most of the important statistical properties of such a surface, which are still of interest in the field of contact mechanics. Reference to fractals was not made in this early research, as the concept of fractal dimensions was brought to the attention of a broader public only in 1967 [5]. The recognition of the fact that many engineering surfaces show fractal characteristics affects the aforementioned analyses in several ways. Greenwood concluded that for a fractal surface, one point out of three would become an asperity [6] (this effect is seriously mitigated if two-dimensional height maps are considered instead of linear roughness profiles). The model by Archard, on the other hand, is fractal but not stochastic. Finally, the statistical analysis by Longuet-Higgins relies on the existence of the image moments of the power spectrum of the surface. For fractal surfaces, which are non-stationary random processes, these moments do not exist, corresponding to the fact that statistical parameters such as the root mean square (RMS) roughness depend on the size of the measured area (for a finite measured or simulated area, this inconvenience does not generate any practical problems).

While the fractal nature of surfaces may affect classical models to some degree, the known properties of the statistical functions describing them, such as the power spectrum and autocorrelation function open the possibilities for formulating mathematical models which take this aspect into account, as was done by Majumdar and Bhushan [7,8] for elasto-plastic materials and by Persson for viscoelastic materials [9,10]. However, such models often include additional assumptions in the calculations which affects their mathematical soundness and to some degree their precision [11]. An exception is the mathematical analysis of the contact of the Weierstrass profile [12], but this result is limited to the two-dimensional case.

As a consequence, most researchers try to incorporate the fractal nature of surfaces through numerical simulation of both the fractal surface and the contact problem [7,13,14]. It shall be noted that often, such simulations are based on surface profiles obtained along a line and not on the entire measured or simulated surface, which is the topic treated in this paper. In some occasions, complete surfaces are generated, but only to extract a large number of linear scans for statistical analysis [15-17]. Taking into account the widespread availability of fully 3D optical profilers which provide complete height maps, such approaches are becoming more and more anachronistic.

Full 3-D analysis has received more attention in recent times. On the one hand, there are improved versions of the original GW-model [18,19], on the other hand, large-scale numerical methods are used by means of finite elements [20,21], boundary elements [22-24], and combinations of various techniques in a multiscale approach [24,25]. The main complication associated to these simulations is the elevated computational cost associated to the solution of large systems of equations or to the iterations required for incremental solutions. Very specifically, Putignano et al. [22-24] describe the need for mesh refinement to acquire numerical

convergence, i.e. they investigate the point to which the mesh must be locally refined beyond which no significant increase in precision is obtained.

The present work takes an entirely different approach to the problem of convergence. While some finite element results will be presented to illustrate the problems to be addressed, the focus of the text is on the statistical aspects introduced by the measurement or simulation of random surfaces. A single example of a measured surface will be compared by simulated surfaces produced by the midpoint algorithm (MP), the random spectral method (RS) and the generalised Weierstrass-Mandelbrot (WM) function, as explained in section 2. The geometrical characteristics used to analyse these surfaces will be outlined and illustrated by an example of each of the techniques proposed. Then, a statistical analysis will be presented of some of these characteristics made on 100 repetitions for the MP and RS methods. To clearly exemplify the importance of such analysis in contact mechanics, a numerical version of the GW-model is applied to each of the simulated surfaces and the statistics of the results will be analysed.

2 METHODS

Three methods were considered to create the randomly rough surfaces. The first one is the random midpoint algorithm with random additions only to the midpoints, as described by Saupe [26] and used in contact simulations by Hyun et al. [20,21]. The second method (RS) is based on the analysis of random surfaces by Longuet-Higgins [4], who analised surfaces produced by an infinite cosine series where the amplitude of the terms in the series scales as a known function (the power spectrum) of the wavelength and the phase angles are randomly distributed in the interval [-π,π]. The method is described by the following formula:

$$z(x,y) = \frac{2\pi(b-a)}{N}\sum_{n=1}^{N} c(r)\cos[r(2\pi x\cos\theta + 2\pi y\sin\theta + \varphi)]$$

where z is the surface height, N the number of terms in the series, r the length of the wave vector, a and b the lower and upper cut-of length for the wave vector, θ the angle between the wave vector and the X-axis and φ a random phase angle. The amplitude $c(r)$ obeys the following law:

$$c(r) = r^{-7+2D}$$

The angles θ and φ are randomly chosen in the interval [-π,π]. The value of r is randomly chosen in the interval $[a,b]$ in such a way that the wave vectors are uniformly distributed in frequency space. D is the fractal dimension. All results in the present work correspond to N=1000.

For the WM-surface, the following formula is used [13,14,27]:

$$z(x,y) = L\left(\frac{G}{L}\right)^{D-2}\sqrt{\frac{\log\gamma}{M}}\sum_{m=1}^{M}\sum_{n=0}^{N}\gamma^{(D-3)n}\cos\Big[\varphi - \cos\left(2\pi\gamma^{n}\sqrt{x^2+y^2}\cos\left(\arctan\left(\frac{y}{x}\right)-\frac{\pi\, m}{M}\right)\right)+\varphi\Big]$$

L is the length of the simulated surface, which is taken equal to 1 in this work. G is called the fractal roughness. The lacunarity γ [26] was set equal to 1.5 as suggested in literature [7]. The random angle φ is chosen from a uniform distribution on [-π,π]. M is taken equal to 9 and N=14.

All surfaces were calculated on a unit square with 256×256 subdivisions. The upper and lower cut-off for the RS method were taken equal to 1 and 2^8 respectively. The mean value of the simulated height was subtracted from the height values in each point and the height values

divided by the standard deviation. Therefore, all surfaces have the same RMS roughness of 1. The power spectra were calculated as the absolute value of the Fourier transform of the surface. In each point, the derivatives were determined by fitting the following polynomial to the point and 8 surrounding points (neighbours and corners):

$$f(x,y) = f(x_0,y_0) + f_{10}(x-x_0) + f_{01}(y-y_0) + \frac{f_{20}}{2}(x-x_0)^2 + f_{11}(x-x_0)(y-y_0) + \frac{f_{02}}{2}(y-y_0)^2$$

The f_{ij} in this formula evidently are the first and second partial derivatives of the function in the neighbourhood of the point (x_0,y_0). Asperities were determined as points which were higher than the eight surrounding points. The asperity radius was calculated as the geometric mean of the eigenvalues of the Hessian at the corresponding point. The fractal dimension of the surface was calculated by the triangular prism method [28,29].

To illustrate the relevance of statistical variations in the field of contact mechanics, a numerical version of the GW-model (nGW) was used for each simulated surface. Load and contact area are calculated for each individual asperity by first defining the impression depth of an asperity:

$$h_i(z) = \begin{cases} z_0 - z & z < z_0 \\ 0 & z \geq z_0 \end{cases}$$

where z_0 is the original vertical position of the asperity and z the actual position of the contacting plane. Then the load and contact area of an individual asperity are given by:

$$p_i(z) = \frac{4}{3} r_i^{1/2} h_i^{3/2}$$

$$a_i(z) = \pi r_i h_i$$

and the evolution of the total load and area are simply obtained by summing the above formulas for all asperities at a given number of discrete values for z. In the results, non-dimensional areas (contact area / total area) and non-dimensional loads (total load × total area / Young's modulus) are used. As a consequence of setting the standard deviation of the roughness to 1 (for an area of 1×1), the roughness studied here is very high as compared to what is found on engineering surfaces, but this artefact is not relevant for the results.

Although the main topic of this paper relates to the statistics of surfaces generated by numerical algorithms, a brief reference will be made to a measured surface and to the finite element modelling of contact problems to provide a reference and justification for the study. The measured surface was arbitrarily chosen from a set of available results obtained in a NANOVEA white light achromatic optical profiler and corresponds to a cold-rolled and recrystallised AA6016T4 aluminium alloy. This material is intended for deep-drawing applications in the automotive industry but is not subject to a specific surface modification process and therefore shows a fractal roughness pattern, inherited from the roughness of the rolls.

A finite element mesh was generated in ABAQUS which has 244×244 (3^5+1) surface nodes. Three layers of uniform cube elements are used underneath the surface before the mesh is allowed to coarsen with a factor of 3 in each subsequent two layers of elements below the surface. All the important stress concentrations during the simulations are limited to the upper three, fine-meshed layers of the model. The simulations were performed under an explicit integration scheme; care was taken to maintain the kinetic energy of the model below 5% of the total energy and to avoid dynamic effects at the moment of first contact between the bodies.

Roughness was introduced on the surfaces of both contacting bodies by means of the MP-method with a RMS roughness equal to 1/10 of the element height in the upper three layers of the model. The upper contacting body was modelled as an elastic solid with a Young's

modulus of 210 GPa and Poisson coefficient of 0.3, the lower body had the same elastic properties but was assigned a yield stress of 210 MPa and a strain hardening exponent of 0.2, using Hollomon's equation for the elastoplastic contact simulations. The friction coefficient between both surfaces was set equal to 0 in one set of simulations and to 0.1 in a second one, to study the interaction between this effect and the effect of plastic deformation of the asperities. Simulations were executed by approaching both surfaces to a distance equivalent to a bearing area of 40% and then sliding horizontally at a fixed vertical distance.

3 FINITE ELEMENT RESULTS

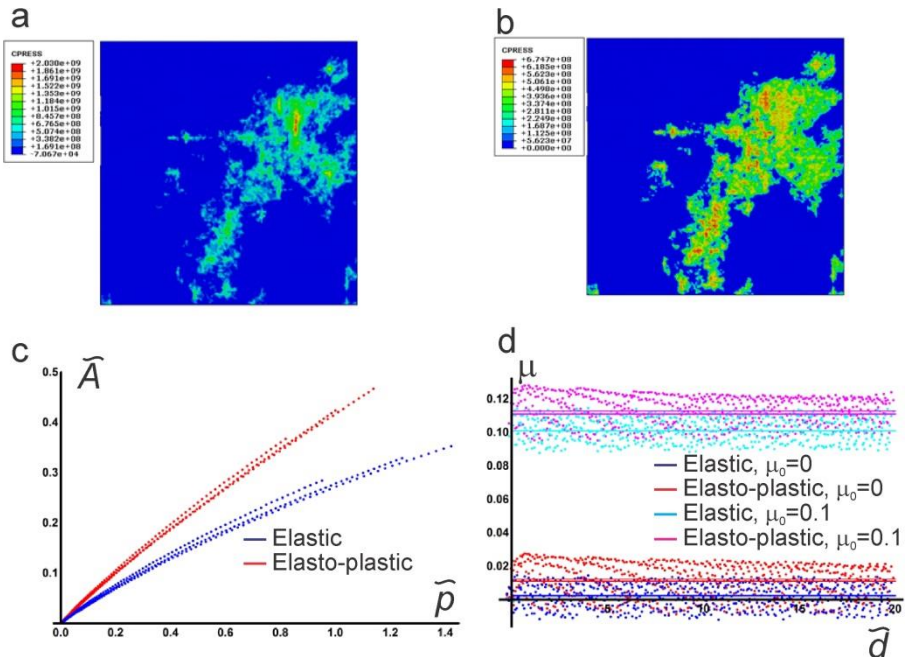

Fig. 1. a) contact area for a fractal surface generated by the midpoint algorithm at 40% bearing area for an elastic and b) elastoplastic strain hardening medium. c) presents the load-displacement curve, d) gives the friction coefficient for movement in the horizontal direction for the elastic and elasto-plastic models at 40% bearing area. The friction coefficients used between the contacting surfaces in the FEM were 0 and 0.1; for the elasto-plastic contact, the resulting friction coefficient is increased due to energy dissipation in the plastic asperities.

The finite element results are discussed first because they illustrate the reason why the statistical simulations are essential. Elastic simulations take approximately four hours on a on a workstation with an Intel® Xeon® CPU E5-2687W processor at 3.40GHz and 64 GB RAM, plastic simulations twice that time, with the horizontal sliding portion representing the main portion of the calculations. The difference in contact area between the elastic (Fig 1a) and elasto-plastic simulations is evident in the load-contact area curves as well (Fig. 1c), with the area increasing more rapidly for the latter case. The effect of the statistical nature of the simulations is clearly visualised in the spread on the curves in Fig. 1c.

One of the long-term goals of the authors is to research the interaction between the friction coefficient μ used in the finite element model (which can be considered as a micro-friction coefficient at the level of the individual asperities) and the one obtained by dividing the horizontal force during sliding by the vertical force (a macro-friction coefficient at the level of the entire body). This is illustrated in Fig. 1d. Here, a very large dispersion is observed in the individual points of the distinct simulations, as the interaction between individual asperities is visualised during the sliding process. The average values differ relatively less but show clear

variation from simulation to simulation. It is also clear that anisotropy of the surfaces would affect the results in sliding, even though its effect in normal contact may be minor.

4 SURFACE SIMULATIONS

Fig. 2 presents graphical examples for individual surfaces. The standard deviations for the height distributions have been scaled to 1 and the fractal dimension of the simulated surfaces was set equal to the measured one, i.e. D=2.8. As a consequence, the topography of the four examples looks very similar (left hand column). With respect to the power spectra (central column), the "grainy" appearance of the spectrum of the measured surface is important to notice. This appears to be a characteristic of "real" surfaces and is very well reproduced by the MP-spectrum and to a lesser degree by RS. In the latter case, an increase of N increases the similarity with the measured data. The spectrum of the WM-surface shows a deterministic pattern of individual peaks and can therefore not be considered as a realistic simulation of measured data. Finally, referring to the autocorrelation functions, it is seen that the measured surface presents a complex pattern which is not found in the simulated ones. This topic has to be researched further.

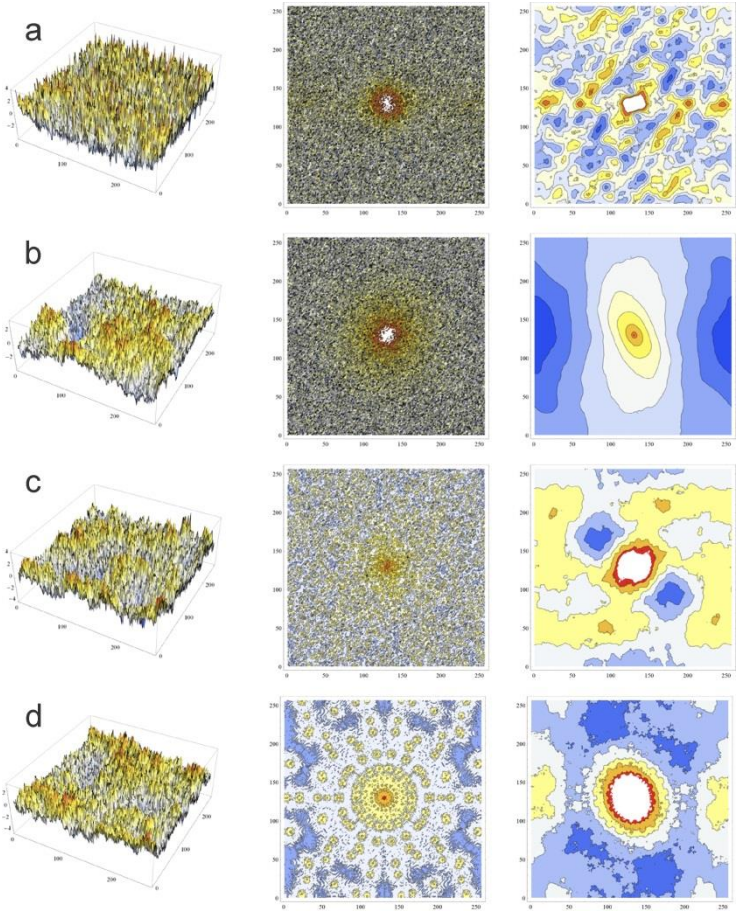

Fig. 2. Graphical representation of the functions describing the surfaces, from left to right the surface topography, the power spectrum and the autocorrelation function for a) a measured surface, b) a surface simulated by the random midpoint algorithm, c) by the random spectral method and d) by the modified Weierstrass-Mandelbrot function.

The statistical characteristics of the four surfaces presented in fig. 2 are analysed in figs. 3-6. Only some of the many possible surface metrics determined during simulation are presented. With respect to the height distributions, height distributions of the asperities and distribu-

tion of the partial derivatives of the surfaces, it is seen that the simulated surfaces follow a Gaussian distribution as predicted by theory [4], while the measured ones do not. Only a slight correlation between asperity radius and height is seen in the measured data, which is almost absent in the simulated ones. In any case, this correlation is probably too weak to be taken into account expressly in contact models. The measured surface is anisotropic, as demonstrated by the difference in the distribution of the partial derivatives and the orientation distribution of the surface gradients. This is a logical result for a cold-rolled and recrystallised material.

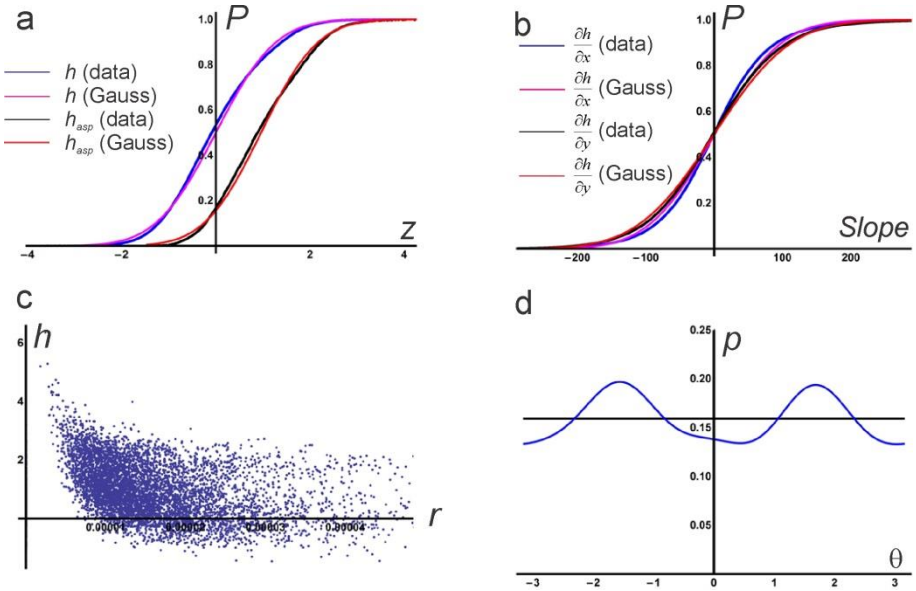

Fig. 3. Statistical parameters of measured surface. a) gives the cumulative distribution function (cdf) of the surface height (all points) and asperity height as well as the ideal cumulative Gaussian distribution with the same mean and standard deviation. b) shows the cdf of the partial derivatives, c) plots asperity heights vs. asperity radius and d) shows the porbability density function (pdf) of the directions of the gradients.

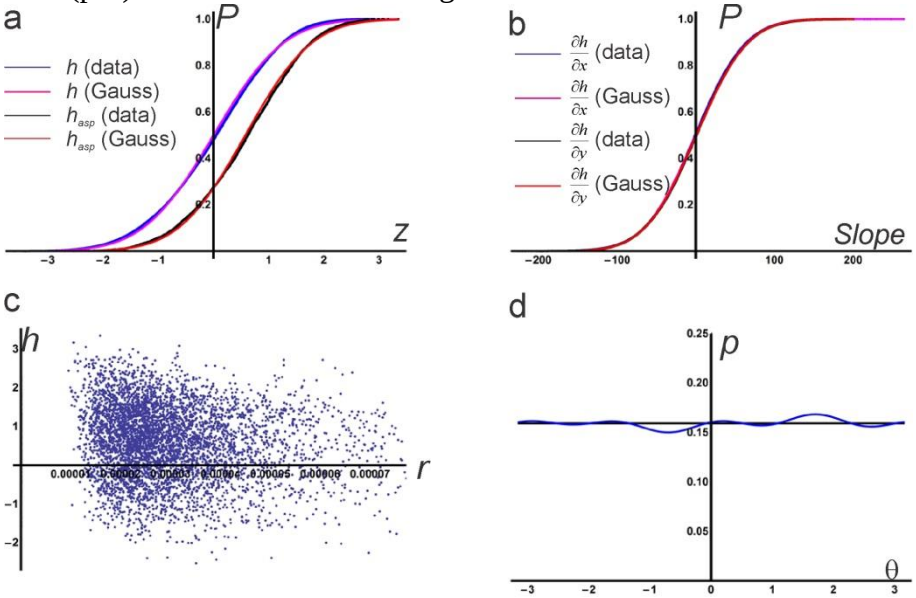

Fig. 4. Statistical parameters of a surface generated by the midpoint algorithm. a) gives the cdf of the surface height (all points) and asperity height as well as the ideal cumulative Gaussian distribution with the same mean and standard deviation. b) shows the cdf of the par-

tial derivatives, c) plots asperity heights vs. asperity radius and d) shows the pdf of the directions of the gradients.

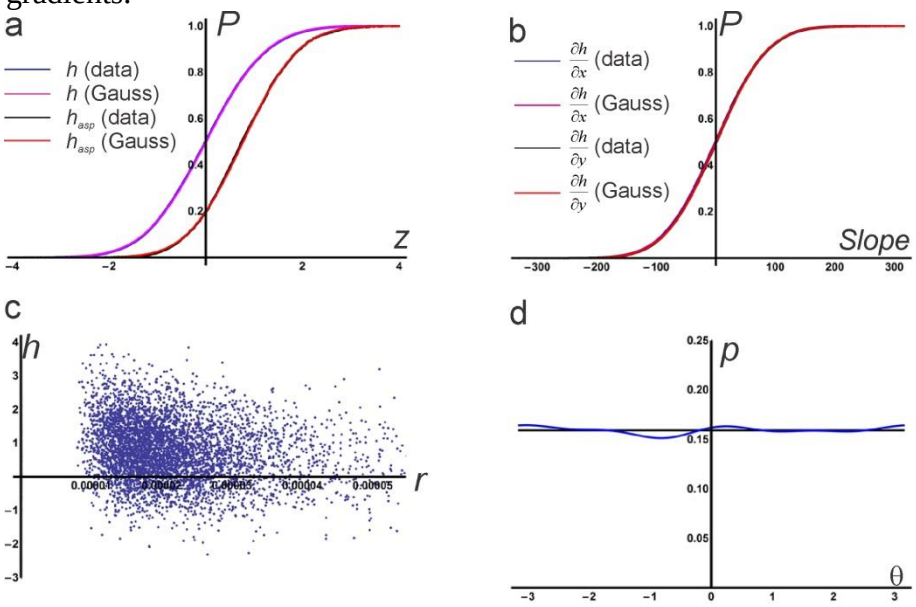

Fig. 5. Statistical parameters of a surface generated by the random spectral method. a) gives the cdf of the surface height (all points) and asperity height as well as the ideal cumulative Gaussian distribution with the same mean and standard deviation. b) shows the cdf of the partial derivatives, c) plots asperity heights vs. asperity radius and d) shows the pdf of the directions of the gradients.

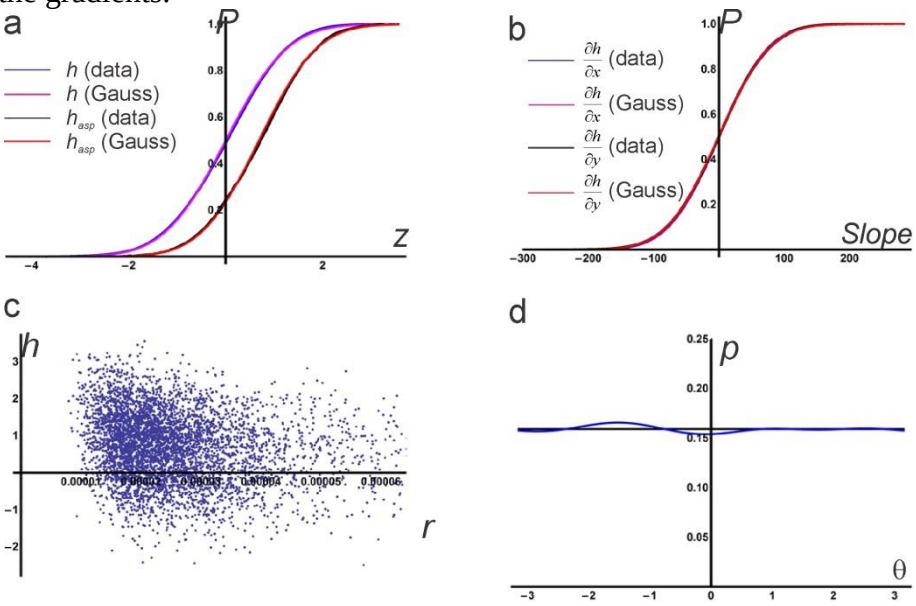

Fig. 6. Statistical parameters of a surface generated by the generalised Weierstrass-Mandelbrot function. a) gives the cdf of the surface height (all points) and asperity height as well as the ideal cumulative Gaussian distribution with the same mean and standard deviation. b) shows the cdf of the partial derivatives, c) plots asperity heights vs. asperity radius and d) shows the pdf of the directions of the gradients.

5 STATISTICAL RESULTS

Results for the statistical simulation of 100 surfaces by the MP and RS methods are analysed here, using a fractal dimension D=2.5. Both the algorithms used for the calculation of the surface as the triangular prism method for the determination of its fractal dimension can induce systematic or statistic variations of the fractal dimension D, as illustrated in fig. 7. The results are biased toward higher values of D and show some variation with respect to the average value. It would certainly be interesting to research the origin of the bias, but the statistical spread is probably a natural result caused by the random nature of the processes involved. It must be compared in future research to the variation observed on real surfaces.

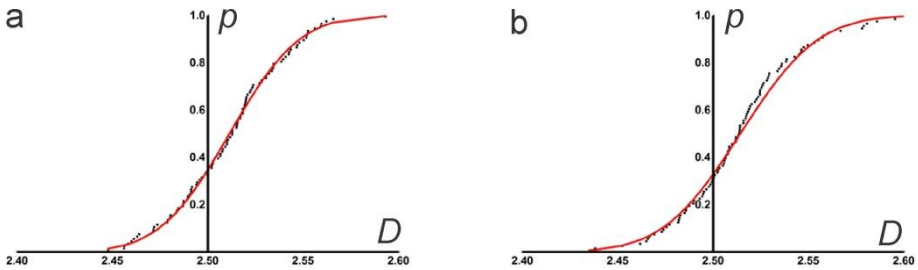

Fig. 7. a) Distribution of the fractal dimension for 100 simulations by the MP-method and b) for the RS-method. The Gaussian distribution is superimposed as a reference.

To illustrate the effect of random variation in the field of contact mechanics, 20 simulation points obtained by the nGW-model for each of the 100 surfaces are plotted in fig. 8. Considerable spread is observed around the average curves. Differences between the average curves are small; to identify such differences quantitatively, more simulations are required to allow determining confidence intervals as a function of the number of simulations.

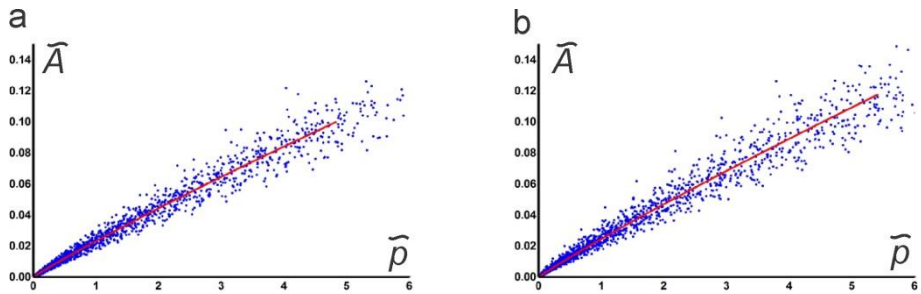

Fig. 8. Results of the nGW-calculations on 100 surfaces simulated by a) the MP-method and b) the RS-method. The red line provides the average of all simulations.

6 SUMMARY AND CONCLUSIONS

- Based on the observation of simulated surfaces alone, the three surface generation algorithms studied here cannot be distinguished and produce isotropic surfaces with a Gaussian distribution of heights and asperity heights. It shall be noted that the experimental measurement used as an example in this paper was anisotropic and showed non-Gaussian distributions, indicating that the fact that the simulated surfaces follow predicted theoretical behaviour does not mean that they are a realistic representation of physical surfaces.
- The random midpoint algorithm produces a power spectrum which closely resembles the power spectrum of measured surfaces and does not show individual frequency peaks. The random spectral method is capable of producing similar spectra if a sufficiently high

number of harmonic components is used. The power spectrum of the bivariate generalised Weierstrass-Mandelbrot surfaces is unrealistic. This is not a problem for contact models which neglect the spatial correlation of the contact areas, such as the Greenwood-Williamson model but may severely affect more advanced models. Moreover, the calculation of the Weierstrass-Mandelbrot function is numerically inefficient: with only 126 harmonics, it requires three times more computation time than the random spectral method with 1000 harmonics. This function should therefore not be used in contact simulations. The midpoint algorithm is more efficient than the spectral method, but may introduce anisotropy effects which have to be further investigated before final conclusions can be reached.

- Although the numerical Greenwood-Williamson model used in this paper is primitive as compared to the standards of modern contact mechanics, it allows identifying the essential phenomena with respect to the problem of statistical variation. Considering the spread on the results, one may consider using less precise methods for contact simulations and instead focus on a higher number of simulations, as long as these are unbiased with respect to the average values obtained. Alternatively, one may increase the size of the simulated surface to capture a wider range of random features and therefore obtain a better average. However, considering that the surfaces studied are non-stationary random processes, increasing the size will also increase statistical variation, while computational cost may increase in a non-proportional manner. This is a topic which has received very little attention and must be addressed in future research.

ACKNOWLEDGMENTS

Financial support of DGAPA under grant IN114215 is acknowledged. The authors wish to thank Miguel Silva and Christian Daniel Maya who participated as students in various aspects of the present work.

REFERENCES

[1] Archard, J. F. Elastic deformation and the laws of friction. Proceedings of the Royal Society of London. Series A. Mathematical and Physical Sciences, 243, 190-205 1957.

[2] Greenwood, J. A., & Williamson, J. B. P. Contact of nominally flat surfaces. Proceedings of the Royal Society of London. Series A. Mathematical and Physical Sciences, 295 300-319 1966.

[3] Whitehouse, D. J., & Archard, J. F. The properties of random surfaces of significance in their contact. Proceedings of the Royal Society of London. A. Mathematical and Physical Sciences, 316, 97-121. 1970.

[4] Longuet-Higgins, M.S. The statistical analysis of a random, moving surface. Philosophical transactions of the Royal Society A, 249, 321-387, 1957.

[5] Mandelbrot, B. B. How long is the coast of Britain? Statistical Self-similarity and Fractional dimension. Science, 156, 636-638 1967.

[6] Greenwood, J. A., & Wu, J. J. Surface roughness and contact: an apology. Meccanica, 36, 617-630, 2001.

[7] Majumdar, A., & Bhushan, B. Role of fractal geometry in roughness characterization and contact mechanics of surfaces. Journal of Tribology, 112, 205-216, 1990.

[8] Majumdar, A., & Bhushan, B. Fractal model of elastic-plastic contact between rough surfaces. Journal of Tribology, 113, 1-11, 1991

[9] Persson, B. N. J. "Elastoplastic contact between randomly rough surfaces." Physical Review Letters 87 116101, 2001.

[10] Persson, B. N.J. "Theory of rubber friction and contact mechanics." The Journal of Chemical Physics 115 3840-3861, 2001.

[11] Manners, W., and J. A. Greenwood. "Some observations on Persson's diffusion theory of elastic contact." Wear 261, 600-610, 2006.

[12] Ciavarella, M., Murolo G., Demelio G., Barber, J.R. Elastic contact stiffness and contact resistance for the Weierstrass profile. Journal of the Mechanics and Physics of Solids, 52, 1247-1256, 2004.

[13] Yan W. and Komvopoulos K. "Contact analysis of elastic-plastic fractal surfaces." Journal of Applied Physics 84 3617-3624, 1998.

[14] Yin, X., and Komvopoulos, K. An adhesive wear model of fractal surfaces in normal contact. International Journal of Solids and Structures 47 912–921, 2010

[15] Tao, Q., Lee, H.P. and Lim, S.P. Contact mechanics with various models of roughness descriptions. Wear 249, 539-545, 2001.

[16] Zavarise, G., Borri-Brunetto, and Paggi, M. On the reliablility of microscopical contact models. Wear 257, 229-245, 2004.

[17] Kogut, L. and Jackson, R.L. A comparison of Contact Modelling Utilizing Statistical and Fractal Approaches. Journal of Tribology, 128, 213-217, 2006.

[18] Ciavarella, M., Delfine, V., & Demelio, G. A “re-vitalized” Greenwood and Williamson model of elastic contact between fractal surfaces. Journal of the Mechanics and Physics of Solids, 54, 2569-2591, 2006.

[19] Ciavarella, M., Greenwood, J. A., & Paggi, M. Inclusion of “interaction” in the Greenwood and Williamson contact theory. Wear, 265, 729-734, 2008

[20] Hyun, S., Pei, L., Molinari, J. F., & Robbins, M. O. Finite-element analysis of contact between elastic self-affine surfaces. Physical Review E, 70, 026117, 2004.

[21] Pei, L., Hyun, S., Molinari, J. F., & Robbins, M. O. Finite element modeling of elasto-plastic contact between rough surfaces. Journal of the Mechanics and Physics of Solids, 53, 2385-2409, 2005.

[22] Putignano, C., Afferrante, L., Carbone, G., & Demelio, G. A new efficient numerical method for contact mechanics of rough surfaces. International Journal of Solids and Structures, 49, 338-343, 2012

[23] Putignano, C., Afferrante, L., Carbone, G., & Demelio, G. The influence of the statistical properties of self-affine surfaces in elastic contacts: A numerical investigation. Journal of the Mechanics and Physics of Solids, 60, 973-982, 2012.

[24] Putignano, C., Afferrante, L., Carbone, G., & Demelio, G. P. A multiscale analysis of elastic contacts and percolation threshold for numerically generated and real rough surfaces. Tribology International, 64, 148-154, 2013

[25] Anciaux, G., & Molinari, J. F. Contact mechanics at the nanoscale, a 3D multiscale approach. International journal for numerical methods in engineering, 79, 1041-1067, 2009.

[26] Saupe, T. Algorithms for random fractals. In: The science of fractal images, 71-136, 1988.

[27] Ausloos, M. and Berman, D.H. A multivariate Weierstrass-Mandelbrot function. Proceedings of the Royal Society of London A, 400, 331-350, 1985.

[28] Clarke C.K. Computation of the fractal dimension of topographic surfaces using the triangular prism surface area method. Computers & Geosciences, 12, 713-722, 1986.

[29] Zou, G, Lam, N.S.N, A comparison of fractal dimension estimators based on multiple surface generation algorithms. Computers & Geosciences, 31, 1260-1269, 2005.